The design of multicore fiber for high power fiber lasers development

HE JIANLI*
Inner Mongolia University of Science and technology, Baotou 014010, China

Design of evanescent-wave-coupled (EWC) multicore fiber laser based on finite element method was presented. By optimizing design parameters, in-phase mode becomes the unique supermode and therefore exhibits much high coupling strength of about 80%. Fundamental LP_{01} mode with a large effective area of 13063 μm^2, relatively good beam quality factor of 2.64, and small confinement coefficient of 0.003 dB/km corresponding to EWC 19-core fiber, shows much better characteristics than other fibers. Results demonstrate that this structure is proposed to be a potential system for high power fiber laser.

(Received May 19, 2019; accepted February 12, 2021)

Keywords: Multicore fiber, Evanescent-wave-coupled (EWC), Supermode

1. Introduction

Currently, cladding pumped fiber lasers, which use single-core (SC), double-clad ytterbium doped fibers in combination with high-power diode pump technology, can generate output powers at several kilowatts [1-7]. Unfortunately, the output power scalability of SC optical fiber laser is limited by mode area, thermal issues and nonlinear effects, such as stimulated Raman scattering and stimulated Brillouin scattering, four-wave mixing and photo-darkening, etc. [3,5-10]. To overcome these limitations, multicore fibers (MCFs) enlarging the effective mode area (A_{eff}) obtainable via SC geometries were introduced recently [3,11]. Compared with those of SC lasers, thermo mechanical effects are mitigated due to mode field distributed nature of the cores [2-4,11].

Researches on MCFs [11-16] are mainly concentrating on the design and fabrication of: (i) multimodal MCF lasers adopting different in-phase mode (IPM) selection/filtering techniques; (ii) multimodal MCF amplifiers with IPM excitation; (iii) single mode MCFs for laser beam delivering; (iv) cut-off wavelength analysis of rare earth doped single mode MCFs. Inventions of these MCFs have opened new avenues for the design of fiber optic components and devices such as in switching, mode locking, and phase-locked high-power lasers [10-12].

Among those categories above, there are few reports concerning on evanescently coupled MCF spontaneously operated in IPM for high power amplifier system [13]. In the previous days, an optimized evanescent-wave-coupled (EWC) 7-core high power fiber laser system with extremely large output power of 100 W was reported by Cheo *et al.* [14]; in addition, a typical evanescent coupling 19-core hexagonal structure MCF was also demonstrated in a fiber amplifier [15,16], which covers 20 dB gain output and very high beam quality.

In this study, we reported on the design and simulation of EWC 19-core fiber for ultra-high power laser and master oscillator power amplifier (MOPA) system [17-22]. Compared with Ref. 14 and 15, core to core distances of our designed fiber are smaller enough, and therefore higher coupling efficiency of 80%, lager A_{eff} of 13063 μm^2 and unique IPM were obtained. Results indicate that EWC 19-core fiber is a good candidate for ultra-high power MOPA system by combining four critical merits: (i) large A_{eff}, (ii) high beam quality factor β, (iii) low loss α, and (iv) high coupling efficiency.

2. 19-core multicore fiber

MOPA system we designed is shown in Fig. 1. Master Oscillator, coupler, pump lasers, and amplifier are main schemes. Core of signal fiber has a diameter of 20 μm and cladding's is 400 μm. Master Oscillator provides an output power of 1.0 KW at the wavelength of 1080 nm with signal fiber connected to the proposed MCF. Surrounding MCF is six Yb-doped transmitting energy fibers with a cladding diameter of 150 μm which placed on a hexagon as pump ring that seems to be a 'plum flower' as illustrated in Fig. 1. Central core is the designed EWC 19-core fiber demonstrated as follow for details. This pump setup optically multiplexed with six 1.2-KW LDs at ~976 nm in which the whole amplifier system forms a (6+1)×1 fiber combiner to couple pump energy. When slope efficiency of Stokes efficiency limit is as high as 60-70%, maximum output power of the present 6-fiber pump-ring can reach to ~5 KW. Therefore, with this MCF

and pump configuration, ultra-high power fiber laser and MOPA system can be easily come true. In order to achieve the best amplifying result, it is essential to choose the most appropriate parameter of the designed MCF.

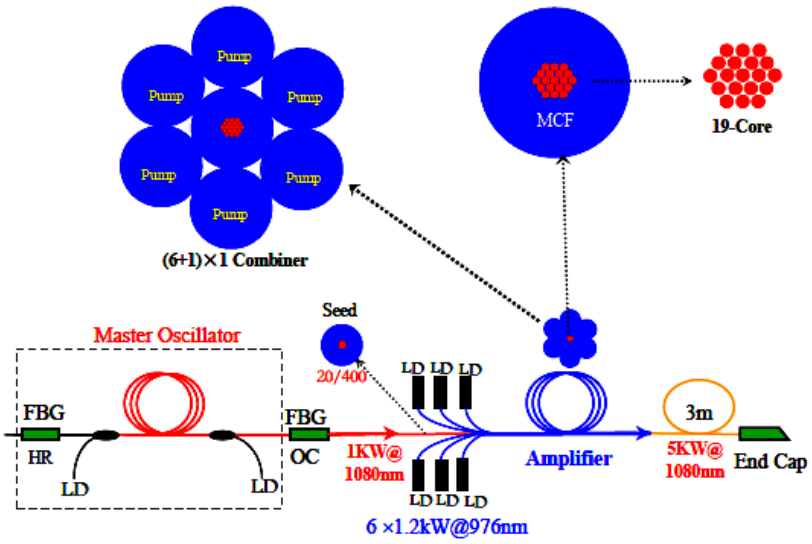

Fig. 1. 19-core MOPA system (color online)

Cores are closed enough to make beam coupled via evanescent wave so that light power can transfer from one core to another. By optimizing the structure of MCF, IPM is obtained finally. Fig. 2 shows refractive index profile of EWC-MCF. Each core has a diameter d_{MCF} of 30 μm with core-cladding index step, Δn, of 1.5×10^{-3} and pump cladding refractive index, n_0, of 1.458. With numerical aperture (NA) of 0.06, core to core distance (Λ_{MCF}) is continuously adjustable, and inner cladding diameter is assumed to be the maximum diameter of hexagon-shaped MCF. Simulating wavelength (λ) is 1.08 μm, and calculated length (L) is set as 90 mm. For simplicity, pump radiation attenuation along the fiber is neglected.

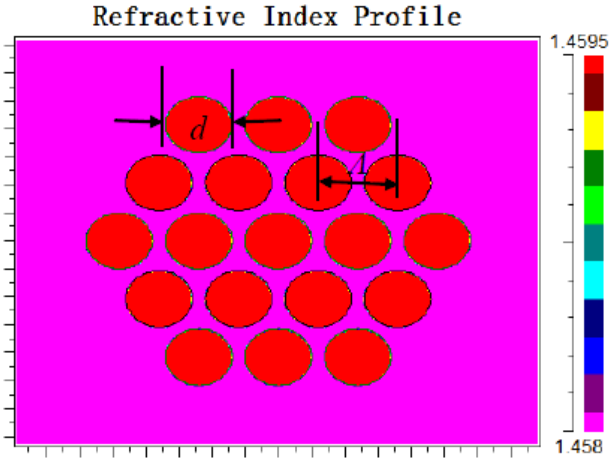

Fig. 2. Refractive index profile of the 19-core fiber (color online)

3. Theoretical mode

We use finite element method (FEM) to numerically simulate characteristics of MCFs. All of the modes and optical fields propagating in these 19 cores are coupled, resulting in what are called supermodes [2,4,13]. Assuming that light propagation in core couples into its nearest neighbors, the distribution of electric field of each core, $E_m(x,y)\exp(i\beta_m z)$, has its own distinctive intensity distribution and diffraction property. The supermode $E(x, y, z)$ can be approximated as a weighted superposition of individual modes [14,16,25],

$$\mathrm{E}^{\nu}(x,y,z)=\sum\nolimits_m A_m(z)E_m(x,y)\exp(ik_m z)$$

$$\mathrm{M}=1,2,\ldots 7 \qquad (1)$$

Coupling model equation can be expressed as [9,12],

$$\frac{\mathrm{dE}_m}{dz}=-ik_m A_m(z)e^{-ik_m z}+\sum\nolimits_m \kappa_{m,n}A_n(z)e^{-ik_n z}, \qquad (2)$$

where $A_m(z)$ is amplitude of field in m_{th} core, n represents number of the nearest neighboring cores, $\kappa_{m,n}$ and k_m correspond to coupling coefficient and propagation constant respectively. $\kappa_{m,n}$ can be expressed by equation [9,12],

$$\kappa_{m,n}=\frac{k_0^2}{2}\int[n^2(x,y)-n_m^2(x,y)]\varepsilon_n^*(x,y)\varepsilon_m(x,y)dxdy \qquad (3)$$

where $n_m(x,y)$ and $\varepsilon_m(x,y)$ are refractive index distribution and normalized electric field distribution, when only m_{th} core is present, $k_0=2\pi/\lambda$ is wave vector in free space, and $n(x,y)$ is refractive index distribution.

Equation (2) can be solved as an eigenvalue problem to find all the 19 supermodes. The 19 eigenvectors consist of weight factors [A_1, A_2,… A_{19}] for each core, and corresponding 19 eigenvalues are propagation constants k of supermodes. k can be arranged in a decreasing order, and in-phase supermode (IPSM), which possesses zero phase difference among all cores, is the first mode because it always has the largest k. Moreover, confinement loss (α_c), which has been described in equation (4), is an important parameter to evaluate the quality of MCF [26].

$$\alpha_c = \frac{20}{\ln 10} \times \frac{2\pi}{\lambda} \times 10^6 \times n_I \qquad (4)$$

where n_I is imaginary part of effective index. Besides α_c, bend loss (α_b) is another significant character for high power laser application [27]. Bent fiber can be treated as a straight fiber with an equivalent index n_{eq} given by Equation (5):

$$n_{eq}^2(r,\varphi) = n^2(r) \cdot (1 + 2\frac{r}{\rho R}\cos\varphi), \qquad (5)$$

where $n(r)$ is index profile of unbent fiber, R is bend radius, φ is azimuth and ρ is a correction due to elasto-optic effect.

4. Results and discussion

4.1. Field distribution

Fig. 3 shows the dependence of near-field intensity on Λ_{MCF}. It can be seen that only the first structure (MCF-30C) presents a same phase distribution. More important to note, only one supermode occurs at the end of MCF facet. This effect, a reduction of supermode modes from 19 to 1, is the result of a strong overlap of wave fields from different cores due to their slight core-cladding index difference [5,16,28]. A great coupling strength of ~80% is thereby obtained. Such design is beneficial for beam coherent combination [11].

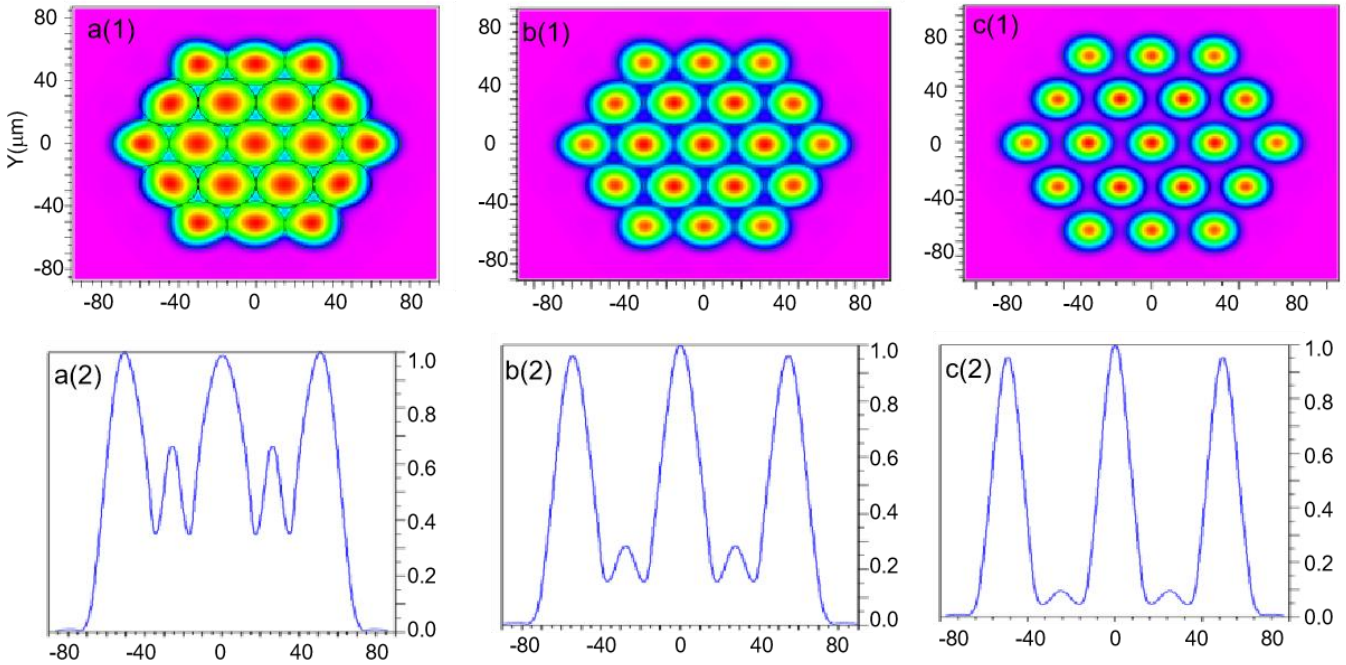

Fig. 3. The near-field intensity distributions depend on Λ: (a) Λ=30 μm (MCF-30C); (b) Λ=32 μm (MCF-32C); (c) Λ=36 μm (MCF-36C) (color online)

To further understand the process of beam coherent combination, signal electromagnetic field distributions for MCF-30C laser simulated at different propagation distances (Z) are shown in Fig. 4 and supplemental material (Media 1) demonstrates dynamic process in detail. As indicated in Fig. 4, energy gathers into central lobe through EWC beam combination and outer 18 lobes become very weak in IPM. Consequently, high beam quality is expected when the central lobe is absolutely dominant. From the Media 1, we can easily see that all the 19 beams almost integrate into ones when propagating distance exceeds 9 mm and then spread out slowly, which results in periodic variation of power. This value significantly shows that the designed MCF-30C fiber is suitable for ultrashort cavity laser and appropriate for amplification of information if the propagating length of light converging is chosen.

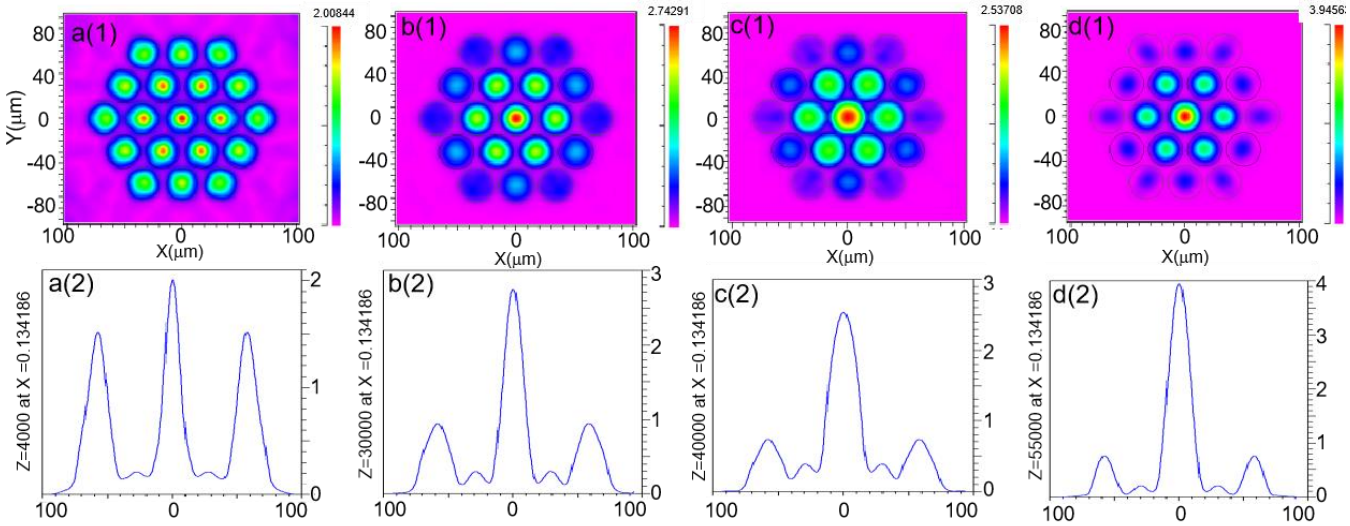

Fig. 4. Beam coupling process in 19-core high power fiber laser system along the propagation way: (a) output Z=4 mm; (b) Z=30 mm; (c) Z=40 mm; and (d) Z=55 mm (color online)

4.2. Characteristics of fiber

In order to evaluate combining effect, beam quality factor β [29] is defined.

$$\beta = \frac{\mathrm{D}}{1.22\lambda}\theta_f , \tag{6}$$

where θ_f is half divergence of far-field (FF), D is defined by the smallest diameter of a circle that contains all the fiber cores. The corresponding results are shown in Table 1. The proposed system as designed for MCF-30C shows an effective beam *N.A.* of 0.0232, approximately one third of that of each single core. It also has a large A_{eff} of 13063 μm^2 (more than 50 times than that of single core) to avoid nonlinear effects and thermo-optical damage. This A_{eff} is very high with neglecting bending losses, fiber inhomogeneity, splicing losses and pump coupling losses.

Table 1. Different parameters of SC and MCF fibers

Sample	D(μm)	ω(μm)	θ_f	*N.A.*	M^2	β	A_{eff}(μm^2)
SC	30	8.5	2.88	0.06	1.242	1.53	227
MCF-30C	150	64.5	1.33	0.0232	4.35	2.64	13063
MCF-32C	158	69	1.53	0.0267	5.35	3.2	14949
MCF-34C	166	75	1.8	0.0314	6.85	3.96	17662
MCF-36C	174	80	1.9	0.0342	7.71	4.38	20096

In general, β is required to be lower than 2 for high power fiber laser system, and it conflicts with the requirement of high A_{eff}. However, high A_{eff} can effectively overcome nonlinear effects and enhance output power, so we consider A_{eff} firstly. Therefore, in our design, it is acceptable that β is higher than 2. Fully considering A_{eff} and β, MCF-30C fiber is proposed to be the most potential material for MOPA system. Fig. 6(c) demonstrates near-field intensity and far-field pattern of output wave field of MCF-30C when Gaussian beam seeds are coupled into the proposed fiber laser system. It exhibits an advantage of obtaining high beam quality laser because the power mostly concentrates in the center of mode field and therefore can operate in its fundamental IPM with a Gaussian beam as a high power seed source [4,10,11].

Fig. 5(a) demonstrates that α_c is as low as ~0.003 dB/km at 1.08 μm for LP_{01} mode, which is helpful to mitigate the background loss of rare-earth-doped MCF for high-power laser application. α_b of MCF-30C versus bending radius is showed in Fig. 5(b). At a bending radius of R=0.20 m, α_b is 9×10^{-4} dB/m with an A_{eff} of 13063 μm^2, whereas the calculated loss of 19-core fiber [30] is 0.6

dB/m (A_{eff}=470 μm^2), not mention to loss of SIF [30]. In general, larger A_{eff} will result in higher bending sensitivity, which indirectly turns out that α_b of MCF-30C is much lower.

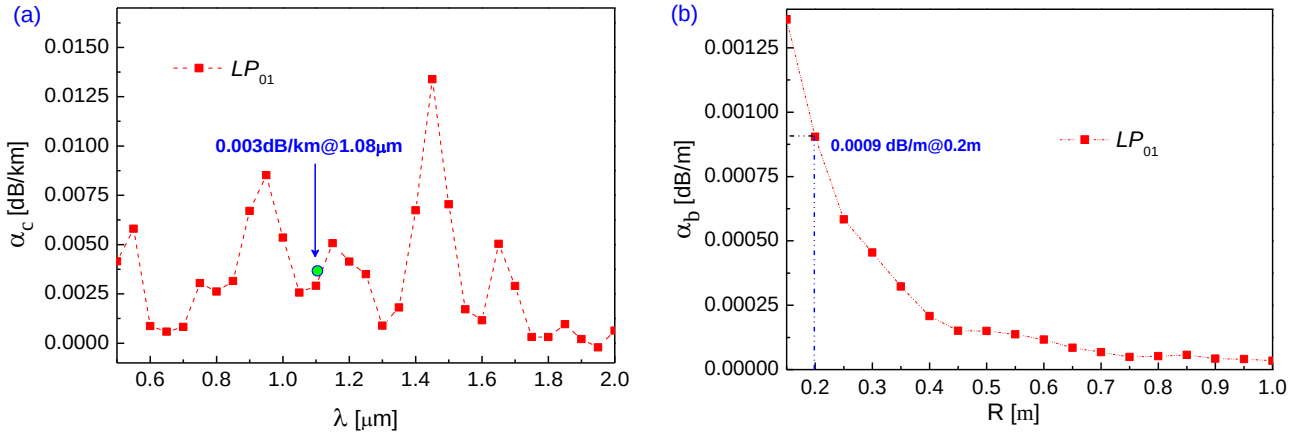

Fig. 5. (a) Confinement loss versus the wavelength; (b) Bending loss versus bending radius (color online)

For the purpose of investigating how the number of cores affects beam properties, we use SC fiber and identical structured parameters of 7-core MCF, displayed in Fig. 6(a) and Fig. 6(b), as references. The comparison results demonstrate that combined beam peak intensity of 19-core fiber is far larger than that of SC fiber. Moreover, the intensity is about 2.5 times of that of 7-core MCF. Results indicate obvious advantages of EWC 19-core fiber over the conventional step-index fiber and 7-core fiber.

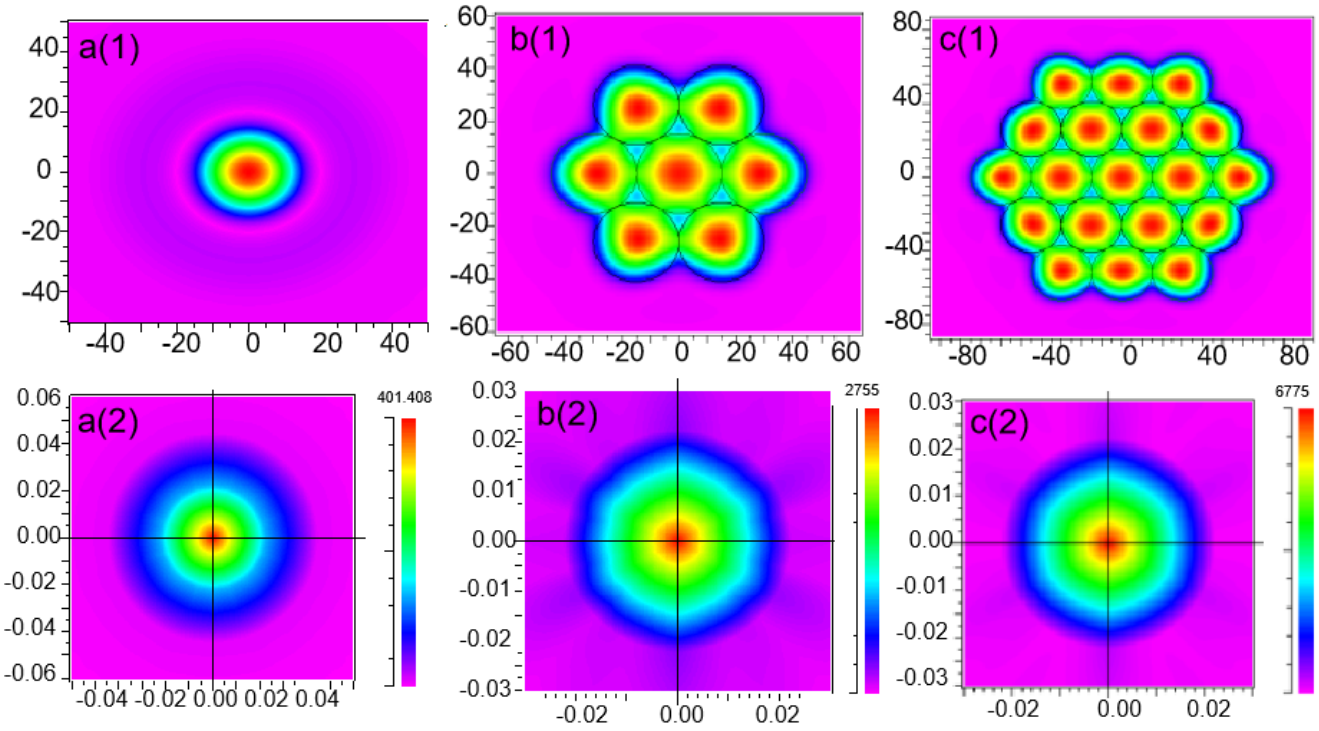

Fig. 6. Near-field and Far-field intensity distributions: (a) Single-core; (b) Seven-core; (c) Nineteen-core (color online)

(6+1)×1 fiber combiner, with one Yb-doped LMA fiber in the central core, has been successfully made by our team. It will be described clearly as soon as possible. 19-core MCF is much more difficult to fabricate compared to Yb-doped single core fiber [31], but as the development of technology, this can be achieved as well. Researchers

from Nufern, East Granby, CT had successfully fabricated the Yb-doped 19-core microstructured fiber [15]. Therefore, the next step for our team is fabricating the designed 19-core MCF by using the standard stack-and-draw technique as Nufern's.

5. Conclusion

In conclusion, EWC 19-core high power fiber laser system was designed and simulated. Analysis parameters are reasonable that effective beam *N.A.* of MCF is 0.0232, both diameters d_{MCF} of each core and core-to-core distance Λ_{MCF} are set to be 30 μm. The proposed MCF possesses extremely large A_{eff} of 13063 μm^2, high coupling efficiency of 80%, and small α_c of 0.003 dB/km. All results demonstrate that EWC beam combination in 19-core fiber result in far-field beam with high brightness and excellent beam quality for ultra-high power MOPA laser system.

Acknowledgments

This work was funded by grants No. 2017MS0109 from Natural Science Foundation of Inner Mongolia Autonomous Region and the Inner Mongolia University of Science and Technology Innovation Fund (Grant No. 2016QDL-B13).

References

[1] I. P. G. Photonics, http://www.ipgphotonics.com/ newsproduct.htm (June 15, 2009).
[2] X. Zhang, X. Zhang, Q. Wang, J. Chang, G. -D. Peng, J. Opt. Soc. Am. A **28**, 924 (2011).
[3] L. Li, A. Zhang, H. Zhan, J. He, T. Shi, Z. Zhou, X. Xiao, A. Lin, Appl. Opt. **52**, 7407 (2013).
[4] C. Wang, F. Zhang, C. Liu, S. Jian, Opt. Express **16**, 5505 (2008).
[5] A. Desfarges-Berthelemot, V. Kermène, D. Sabourdy, J. Boullet, P. Roy, J. Lhermite, A. Barthélémy, C. R. Physique **7**, 244 (2006).
[6] W. Kim, B. Shaw, S. Bayya, C. Askins, J. Peele, D. Rhonehouse, J. Meyers, R. Thapa, D. Gibson, J. Sanghera, Proc. SPIE **9958**, 1 (2016).
[7] Z. Huang, X. Tang, H. Lin, J. Wang, Laser Phys. **26**, 055101(2016).
[8] C. Guan, L. Yuan, J. Shi, Opt. Commun. **283**, 2686 (2010).
[9] S. Liu, S. Li, Chin. Phys. B **22**, 074206 (2013).
[10] X. Fang, M. Hu, Y. Li, L. Chai, C. Wang, J. Lightwave Technol. **29**, 3428 (2011).
[11] H. Wei, G. Zhang, P. Yan, J. Li, X. Zhang, W. Tong, J. Luo, J. Li, K. Chen, in Optical Fiber Communication Conference/National Fiber Optic Engineers Conference 2013, OSA Technical Digest (online) (Optical Society of America, 2013), paper JTh2A.11.
[12] E. J. Bochove, P. K. Cheo, G. G. King, Opt. Lett. **28**, 1200 (2003).
[13] E. J. Bochove, Opt. Lett. **33**, 464 (2008).
[14] P. K. Cheo, A. Liu, G. G. King, IEEE Photon. Technol. Lett. **13**, 439 (2001).
[15] Y. Huo, P. K. Cheo, G. G. King, Opt. Express **12**, 6230 (2004).
[16] A. Schülzgen, L. Li, X. Zhu, V. L. Temyanko, N. Peyghambarian, J. Lightwave Technol. **27**, 1734 (2009).
[17] Y. Li, L. Gao, W. Huang, C. Gao, M. Liu, T. Zhu, Opt. Express **24**, 23450 (2016).
[18] Y. Wang, S. Hu, X. Yang, R. Wang, H. Li, C. Sheng, Photonics Res. **6,** 332 (2018).
[19] Y. Sasaki, K. Takenaga, S. Matsuo, K. Aikawa, K. Saitoh, Opt. Fiber Technol. **35**, 19 (2017).
[20] W. Ren, Z. Tan, Optik **127**, 3248 (2016).
[21] R. Xiao, J. Hou, M. Liu, Z. F. Jiang, Opt. Express **16**, 2015 (2008).
[22] P. Zhou, Y. Ma, X. Wang, H. Ma, X. Xu, Z. Liu, Appl. Opt. **48**, 5251 (2009).
[23] Z. Liu, S. Men, Y. Liu, Z. Cong, H. Yang, W. Cheng, H. Rao, J. Lu, X. Zhang, Opt. Lett. **41**, 1356 (2016).
[24] A. Maleki, M. Kavosh Tehrani, Hossein Saghafifar, M. H. Moghtader Dindarlu, H. Ebadian, Laser Phys. **26**, 025003 (2016).
[25] Y. Huo, P. K. Cheo, J. Opt. Soc. Am. B **22**, 2345 (2005).
[26] J. Sakai, N. Nishida, J. Opt. Soc. Am. B **28**, 379 (2011).
[27] D. Marcuse, Appl. Opt. **21**, 4208 (1982)
[28] N. N. Elkin, A. P. Napartovich, V. N. Troshchieva, D. V. Vysotsky, J. Lightwave Technol. **25**, 3072 (2007).
[29] S. Yi, W. Min, High energy laser system. (National Defense Industry Press, Beijing, 2004), Chap. 3.
[30] M. M. Vogel, M. Abdou-Ahmed, A. Voss, T. Graf, Opt. Lett. **34**, 2876 (2009).
[31] T. Shi, Z. Zhou, L. Ni, X. Xiao, H. Zhan, A. Zhang, A. Lin, Appl. Opt. **53**, 3191 (2014).

*Corresponding author: jianli_he@126.com